ISSN: 0067-2904
GIF: 0.851

# Linking the Timing of Deposition and Organic Matter Richness of the Gulneri Formation of Northern Iraq to the Global Oceanic Anoxic Event 2 (OAE 2): Implications to better constrain the Depositional Models of Iraqi's Oil Source Beds and their Timing of Deposition

**Khedar Ezbar Anazan Al-Sagri***
Department of Geology, College of Science, Baghdad University, Baghdad, Iraq

**Abstract**

Global oceanic anoxic events (OAEs) are events of immense importance for a variety of reasons. For instance, they are not only behind most if not all of the mass extinctions which took place during the Cenozoic era, but they are the harbinger for the world's best oil source beds, which humanity depends on to satisfy its energy need. In spite of this, there was little effort to document their presence in Iraq, to fill in for the void here, and as a first step, this paper will attempt to establish a cause and effect relationship between OAE 2 and the Gulneri Formation timing of deposition and organic matter richness. This was done by showing the prevalent occurrence of the globally known OAE 2 positive $\partial^{13}C_{org}$ excursion and the unique rock-eval fingerprints all through the Gulneri Formation.

The lessons learned are rather many and important. First is the laying down of stringent constraints on the Gulneri Shale age assignment. In view of this study results, this formation age ought to be bracketed between the latest Cenomanian to the earliest Turonian, or in the language number between 93.5 to 93.9 Ma. The second lesson is the gaining of an in-depth expose about the depositional model responsible for making the Gulneri shale to become so rich in organic matter. It is hoped from all of this is to lay down a solid ground for constraining the depositional models of other Iraqi oil source beds.

**Keywords:** OAE 2; global oceanic anoxic event number 2; Gulneri Formation; Iraqi oil source beds

# ربط زمن الترسيب والأغناء بالمواد العضوية لتكوين الكلنيري بالحدث العالمي المحيطي المستنزف للأوكسجين رقم ٢ : معطيات لوضع محددات أفضل للنماذج الترسيبية للصخور العراقيه المولده للنفط وأزمنة ترسيبها

**خضر زبار عنيزان الصكري**
قسم علم الارض، كلية العلوم، جامعة بغداد، بغداد، العراق

**الخلاصه**

الأحداث العالميه المحيطية المستنزفه للاوكسجين ذات أهميه قصوى في تاريخ الارض الجيولوجي، وقد كان الامر كذلك لاسباب عديدة، والتي منها أن هذه الاحداث قد ترابط وقوعها مع جميع ما حدث من هلاكات جماعية للكائنات الحية خلال فترة عصر الحياة الحديثه، وكذلك فأنها الصانعة لأحسن ما هو موجود في العالم من الصخور المصدرة للنفط، ورغم ذلك فأن القليل قد بذل في سبيل توثيق تواجد هذه الاحداث في العراق،

*Email: kbzm5156@yahoo.com

ولغرض ملأ الفراغ الحاصل بهذا الصدد، وكخطوة أولى فأن هذه المقالة ستسعى الى اثبات أن الحدث العالمي المحيطي المستنزف للاوكسجين رقم ٢ هو المسؤول عن ترسيب وأمتلاك تكوين الكلنيري لما هو متميزا به من غناء بالمواد العضوية، وقد جرى توثيق هذه العلاقة من خلال البرهنة على أمتلاك هذا التكوين للخصائص المميزة للحدث العالمي المحيطي المستنزف للأوكسجين رقم ٢، والتي منها وجود البروز العالي لتراكيز نظير كاربون–١٣، وكذلك تواجد خصائص الروك ئيفال المميزة لمقاطع هذا الحدث من أمكان أخرى من العالم. الدروس المستقاة عديده ومهمه، وليس أقلها وضع محددات في غاية الدقة عن عمر تكوين الكلنيري، حيث توصل ان هذا العمر يجب حصره بين أخر السينومنين وأول الترونين، أو باللغة الارقام ما بين ٩٣،٥ – ٩٣،٩ مليون سنة قبل الوقت الحاضر، والدرس الاخر الذي جرى تعلمه هو التوصل الى معرفه عميقه بشأن الكيفية الي صار بها تكوين الكلنيري على ما هو عليه من الغناء بالمواد العضوية، وما جرى التوصل اليه هنا يصلح لأن يكون اساس جيدا لانطلاق الي تطبيقيه على بقية الصخور العراقية الاخرى المصدرة للنفط.

## Introduction

Global oceanic anoxic events (OAEs, henceafter, e.g. [1]) can be defined as causative palaeoceanographic phenomena defining a temporal envelope during which abnormally high amount of organic Carbon ($C_{org}$) or organic matter (OM) had accumulated in marine sediments e.g. [2]. However, the situation is completely the opposite when it comes on how these events are brought about. In spite of the diverse opinion expressed in this regard, there is a wide spread agreement that oceanic warm up brought about by global warming is the triggering event for the OAEs development. According to [3], the causal link between oceanic warming and OAEs development include the following feedbacks: (1) reduced ventilation due to enhanced stratification and weakened circulation; (2) reduction of $O_2$ solubility; (3) increased oceanic fertilization. Each of these feedbacks operates in such away to eliminate $O_2$ oceanic inventory, thereby predisposing the ocean to have one of the OAEs.

When OAEs are well established, they leave diagnostic faunal, lithological, and geochemical imprints on coeval sections of the sedimentary archive. The most important is the mass extinction of existing biomass [e.g. 4-6]. Because these biomass are the main grazer present in the water column, their absence enhances organic matter preservation. A corollary of this is not only the containment of coeval sediments of higher than normal of organic matter concentration, but these sediments and their contained organic matter possession of a positive isotope carbon $^{13}C$ excursion [e.g. 7-8]. This excursion was attributed to the enhanced burial of $^{13}C$ depleted organic matter during the OAEs. The Cretaceous Era (from 65.5 to 144 MA, [9]) had been punctuating by at least ten of the OAEs Figure-1 (e.g. [7]). According to [10], and references therein, the most severe and globally distributed of these is OAE 2, which its time of happening span the Cenomanian-Turonian Boundary Interval (CTBI). As was the case with many of the OAEs, OAE 2 is having a pronounced positive $\partial^{13}C$ excursion of about 2.5% in marine carbonates, and 4 to 6.6 % in organic carbon.

Because the published age of the Gulneri Formation [e.g. 11-13] is very close to that of the OAE 2 time of happening, it seemed very tempting to establish a cause and effect relationship between the two. The theme of this paper is to do so. The benefits and here just to numerate the most important is firstly to improve Iraq's chronostratigraphic framework by stringently constraining the age assignment of the Gulneri Formation. Secondly to have a better idea about how the Gulneri Shale became so rich in organic matter. It is hoped that all of these will help in better constraining the depositional models of the Iraqi oil source beds.

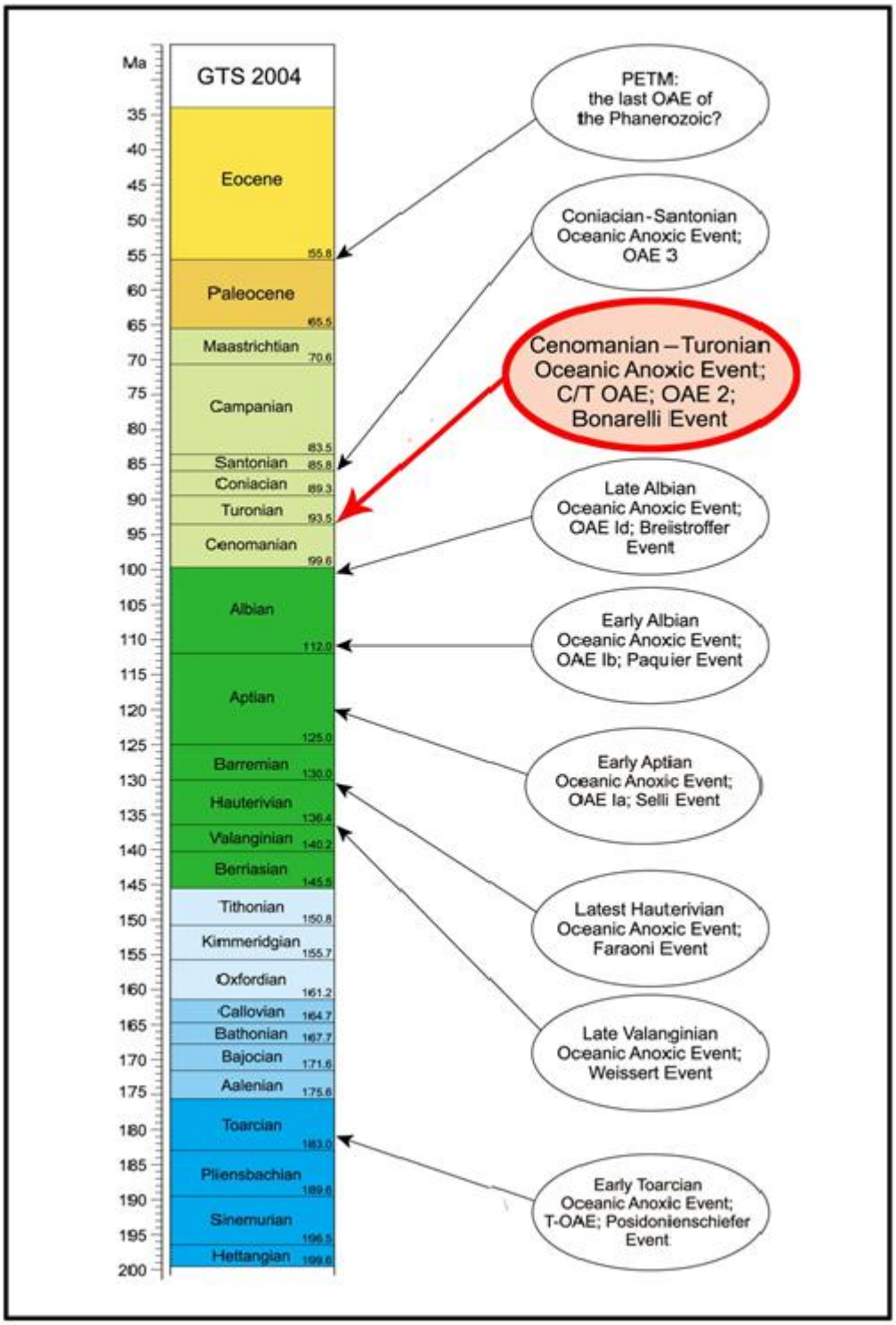


**Figure 1**- generalized columnar presentation for the well identified oceanic anoxic events. Adapted from [7] jenkyns, 2010. The theme of this paper is the cenomanian- turonian oceanic anoxic event or the OAE2.

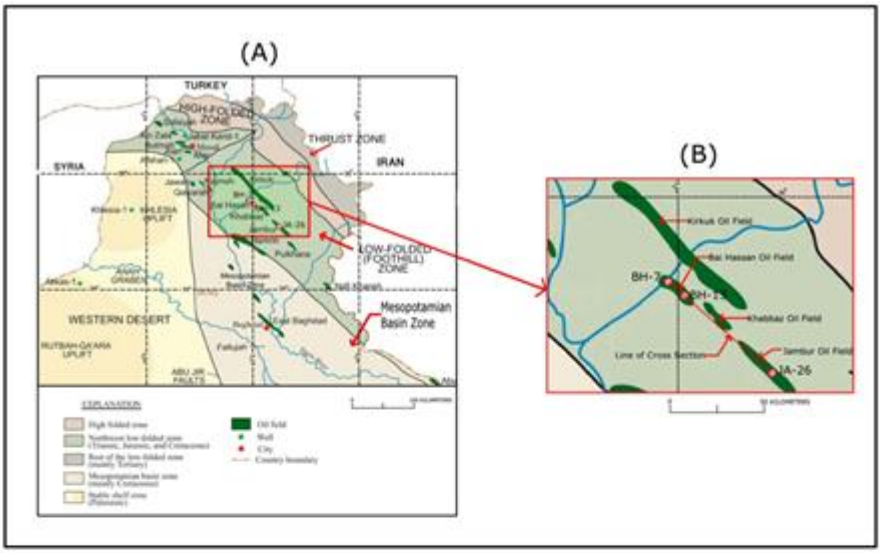


Figure 2; A. generalized geographic setting of the wells from which the studied samples were taken. B. A blown up view for these wells locations. Adapted and modified from [62] Fox and Albran't, 2002.

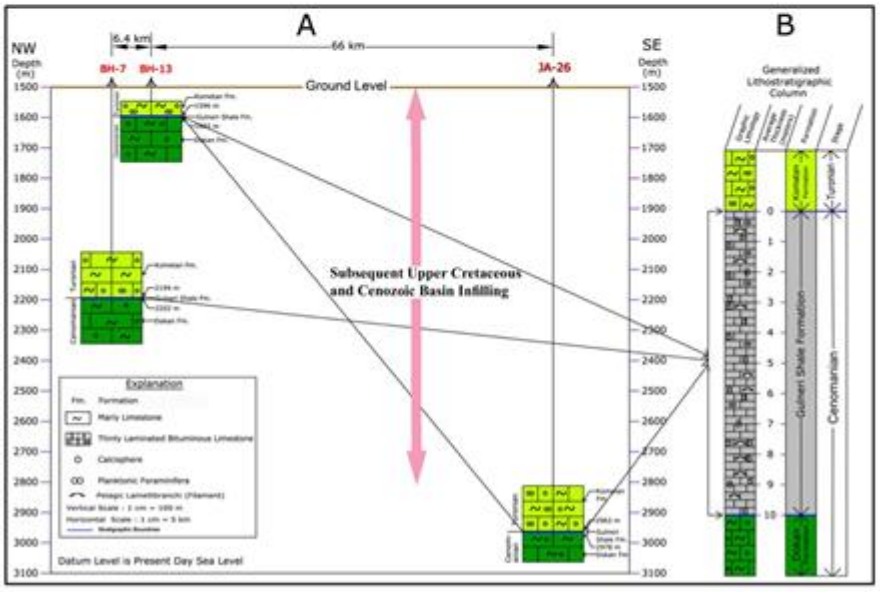


Figure 3. A. Generalized present day structural and stratigraphic setting for the Gulneri Shale Formation in wells BH-7; BH-13; and JA-26. B. detailed lithostratigraphic columnar presentatic for this formation in these wells.

## Geographic and Geologic Setting

### Geographic setting

The rock samples on which this study is constructed are taken from three oil wells, in each of which the Gulneri Shale was cored to a variable depths. The first two are located in Bai Hassan oilfield, namely BH-7 and BH-13. The third one is located in Jambur oilfield, namely JA-26. These wells locations are shown in Figures 2A and B. Furthermore.

### Structure and tectonic setting

Though these oil fields are described as so, they are in fact like many of their alike in northern Iraq, are doubly plunged asymmetrical anticlinal folds, which are more or less arranged into echelon pattern [12], [14]. They all can be categorically described as having long wavelength with low amplitude. [15], and subsequent authors e.g. [16] in their efforts to tectonically zone Iraq, they placed these anticlines into a single zone named as the foothill zone, which is now known as the low-folded zone. The consensus is that this zone as well as Iraq's other zones owe their origin to the rather complex

convergence history between Arabia, and neighboring plates [16-18]. Indeed, this complexity had manifested itself in no better way than in the quite different depths at which the top of the Gulneri Shale was fond in each well, as clearly shown in Figure 3A. For sure, this reflects a different rate of uplift, and or subsidence. However, the author refrains from stepping any further into the issue of why and how the situation was as so.

**Stratigraphy**

The picture here is a bit simpler. In each well, and as shown in Figures 3A and B, the Gulneri Shale is sandwiched between the overlying Kometan Formation and the underlying Dokan Formations. The Gulneri Shale is set apart from these formations because of its distinctive lithology, whereby it's made out of thinly laminated bituminous marly limestone.

Agewise, the age of the Gulneri Shale is traditionally assigned to the Lower Turonian. This assignment was based on the micropaleontological determinations of Bellen et al., 1959. They reported the presence of Rotalipora cf. appeninica Renz; Globotruncana Helvetica Bolli; minute globogerinids; gumbelinids; fish detritus; undetermined small bicarinate. Subsequent work by authors like [12] and [13], had documented the presence of more of the age telling planktic forams, such as heterohelicid; rotaliporad; and whiteinellid. Because such faunal association is known to be the faunal global fingerprints for the OAE 2, as elegantly shown by [19] and [20], the former authors made an excellent case for the Gulneri Shale age to be either very close to the basal Turonian, or be a part of the Cenomain-Turonian Boundary Interval (CTBI) itself. This paper hopes to improve the situation by providing an independent line of inquiry on this issue.

**Samples and Methods**

The samples analyzed to generate the analytical data upon which this study is based are chips cut from the Gulneri Shale cores, which their recovery comes to be about one hundred percent. However, while the coring had entirely penetrated the Gulneri Shale in wells BH-7 and BH-13, it had done so only partially in well JA-26. The sampling interval comes to be about 1.6 meters in wells BH-7 and BH-13, while it was about 0.31 meters in JA-26. These seemingly conflicting facets are all due to different sampling accessibility policies. In the section, a brief mention will be made about the following: the nature of each of the analytical procedure used; definition of output parameters; and whenever possible commenting about each procedure analytical precision.

**Organic carbon isotope ($\partial^{13}C_{org}$)**

A total of 57 samples were analyzed to determine the carbon isotope composition ($\partial^{13}C_{org}$) of their organic carbon fraction. All of these analyses were carried out at the Institute of Earth Sciences of the University of Lausanne, Switzerland, under the supervision of Professor Thierry Adatte. The generated data are reported in the customary delta ($\partial^{13}C_{org}$) notation calibrated against the international standard of Vienna Pee Dee belemnite (VPDB), where $\partial^{13}C_{org}$ (%) = [($^{13}C$ / $^{12}C$) $_{sample}$ / ($^{13}C$ / $^{12}C$) $_{standard}$] X 1000.

Analytical precision was tested by determining $\partial^{13}C_{org}$ of isotopically well characterized lab powder standards. Each of the analyzed samples strings was started and closer by analyzing the same subset of lab standards. Based on these analyses, precision of the $\partial^{13}C_{org}$ data was fond to better than $\pm$ 0.12‰ for each sample (1 sigma or 1 standard deviation). Appendix A gives details of the generated $\partial^{13}C_{org}$ data of the standards and samples daily runs (Table A 1). Appendix B gives details of data precision estimation (Table B 1). Appendix E lists $^{13}C_{org}$ data in their stratigraphic context (Table E 1 for data from well BH-7; Table E 2 for data from well BH-13; and Table E 3 for data from well JA-26).

**Rock-Eval Pyrolysis**

A subset of 56 samples was pyrolized to determine their rock-eval parameters. Again, these analyses were all carried out at the Institute of Earth Sciences of the University of Lausanne, Switzerland under the supervision of Professor Thierry Adatte. The generated parameters include eight, but this paper concern will be only with two of them. The first is total organic carbon or TOC, which is expressed as wt.%. The second is the Hydrogen Index or HI, which is define as ($HI=S_2/TOC \times 100$) in milligrams (mg) of hydrocarbons per grams (g) of TOC, where $S_2$ corresponds to pyrolitically generated hydrocarbons per one gram of rock.

Analytical precision was tested by duplicate analyses of the same lab powder standards (IFP: Toarcian Black Shale). The overall all parameters precision was fond to be better than ±1.72% (1 sigma or 1 standard deviation) for each sample. Appendix C tabulates the daily runs analyses for

samples and lab powdered standards (Table C 1). Appendix D gives details of the precision estimation (Table D 1). Appendix E lists the gathered data within their stratigraphic context, Table-E 1 for data from well BH-7; Table-E 2 for data from well BH-13, and Table-3 for data from JA-26.

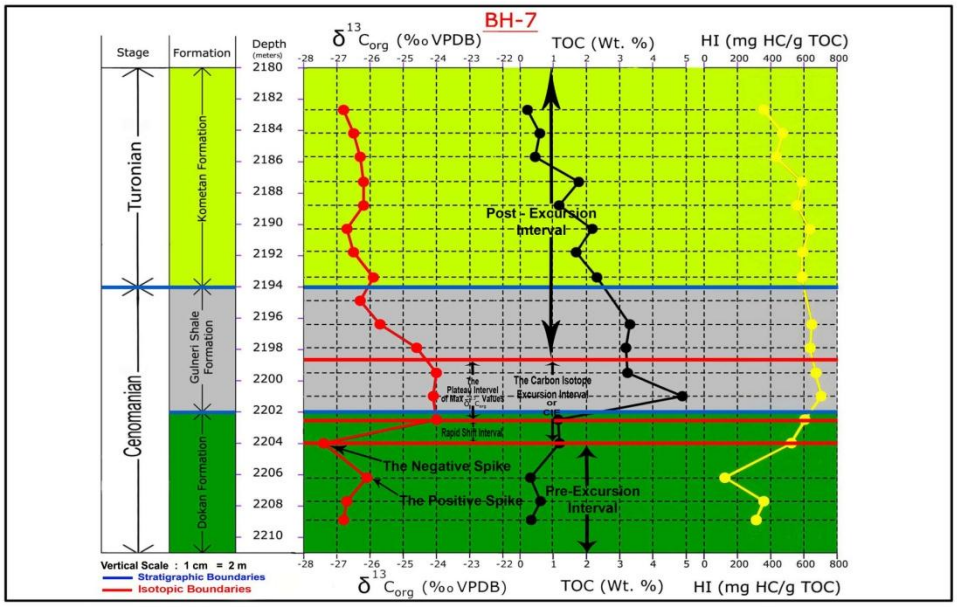


Figure 4. Graphic display for the stratigraphic variability of ∂13Corg; TOC; and HI data for the samples from BH-7.

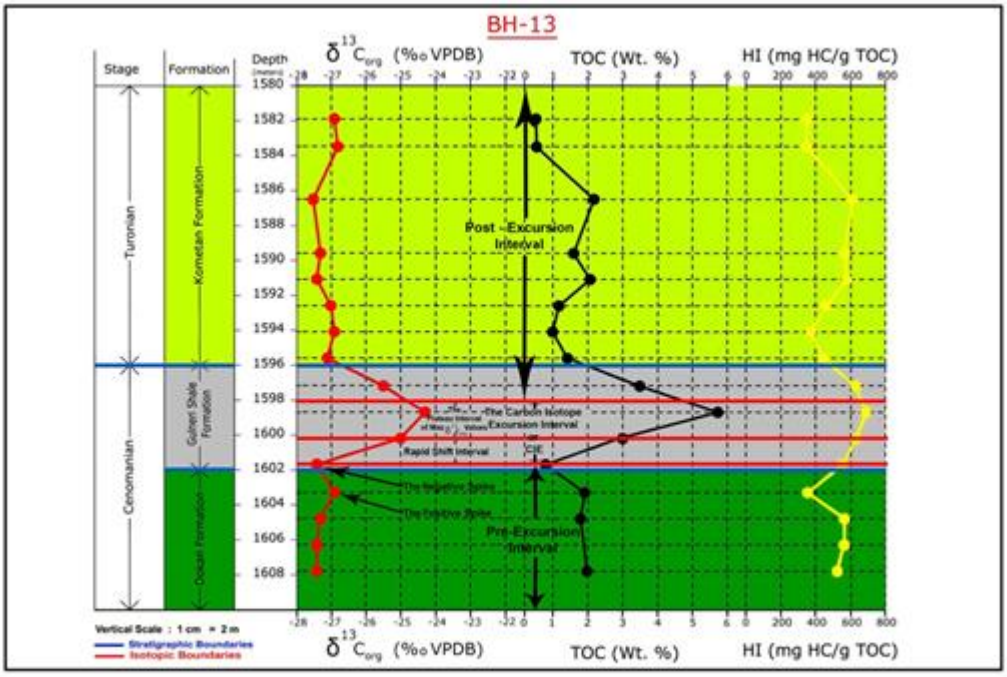


Figure 5; the same as Figure 4, but for samples from well BH-13.

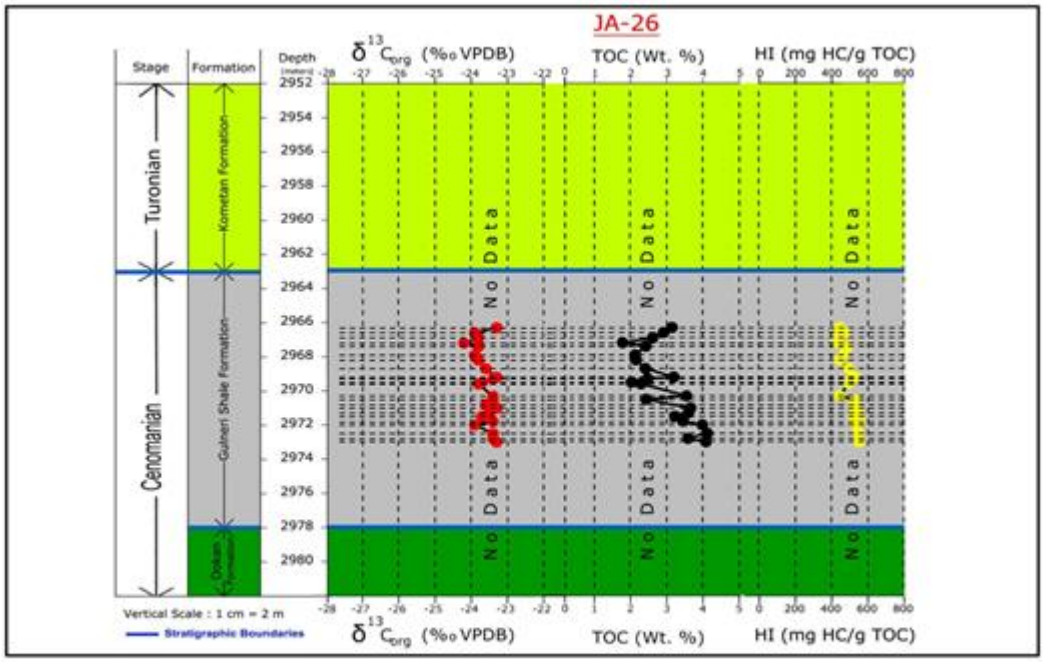


Figure 6. The same as in Figure 4, but for samples from well JA-26.

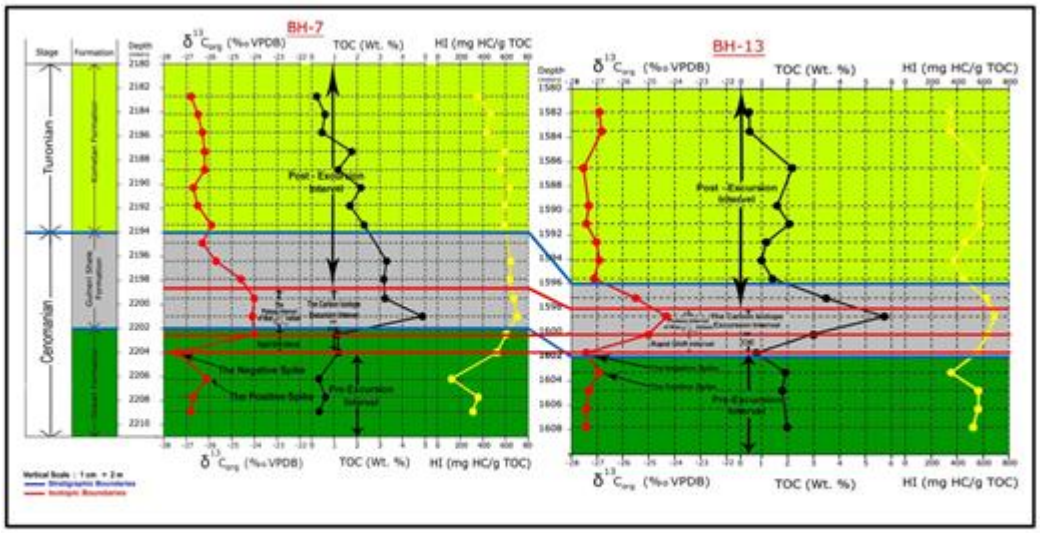


Figure 7. Correlation of ∂13Corg; TOC; and HI records of wells BH-7 and BH-13.

**Results**

The aforementioned data are graphically summarized in Figures 4 to 6. While these figures are an individual portrayal for each well data, Figure-7 is an attempt to correlate the data from wells BH-7 and BH-13. In what to come hereafter, a brief mention is to be made about how $\partial^{13}C_{org}$ ; TOC%; and HI data behave stratigraphically in each well, and how this behavior correlates in moving from one well to another. In so doing, emphasis will not be not only on the nudges and peaks, but also on the interludes as well. Before starting, it must be mentioned that data from JA-26 will not be dealt with any further because of their limited core coverage.

**$\partial^{13}C_{org}$ data**

Based on $\partial^{13}C_{org}$ stratigraphic behavior in each well, and based on these behavior similarities, the section covered by the data was dissected into three sections. They are in ascending order, the lower pre-excursion interval; the middle positive carbon isotope excursion interval (CIE); and the upper post-excursion interval Figures -4 and -5. In wells BH-7 and BH-13 wells, and throughout the pre-excursion interval, $\partial^{13}C_{org}$ data define an upward trend of slight increment starting from values of -26.8‰ in BH-7, and -27.4‰ in BH-13. In either case, the trend culminates at the positive spike,

whereby $\partial^{13}C_{org}$ attains values of -26.1‰ in BH-7, and -26.9‰ in BH-13. Then $\partial^{13}C_{org}$ dips to the lowest values ever recorded in both wells, which happened to be the same (-27.4‰) in both wells. The level of these values was termed the negative spike.

Strikingly, and in both wells, the onset of the positive carbon isotope excursion interval is characterized by rapid positive shift reaching value of -24.0‰ in BH-7, and -25.0‰ in BH-13. The interval from these data points and the negative spike onset were dubbed as the rapid shift interval, which happened that in both wells to have similar thickness. Upsection, there comes the plateau of maximum $\partial^{13}C_{org}$ values, where $\partial^{13}C_{org}$ values fluctuate between -24.0‰ to -24.1‰ in BH-7, and between -25.0‰ to -24.3‰ in BH-13. In addition, it may be noticed that while the plateau thickness is about 5.3 meters in BH-7, it is only 2.2 meters thick in BH-13.

Moving further upward, $\partial^{13}C_{org}$ values decreases progressively throughout the post-excursion interval. That is from -26.3‰ to -26.8‰ in BH-7, and from -25.5‰ to -26.9‰ in BH-13. Also noticeable is the rate at which this decline is happening in either well. While the trend was somewhat gradual in BH-7, it is rather happening at a faster rate in BH-13. Furthermore, $\partial^{13}C_{org}$ values continue to fluctuate up and down through the post-excursion interval of BH-7. The opposite was observed through this interval of BH-13, whereby $\partial^{13}C_{org}$ tend to define a more or less a flat pattern.

**TOC and HI data**

Overall, and in general, these data exhibit stratigraphic trends and patterns similar to those described above. For instance, TOC and HI values show sharp increase in traversing the boundary from the pre-excursion interval to the components of the positive-CIE (carbon isotope excursion) interval. The mean TOC percentage of the latter interval is averaged 2.73% for BH-7, and 3.14% for BH-13. A much lower values were documented for the pre-excursion interval (0.43% for BH-7, and 1.53% for BH-13). The HI values exhibit a more or less similar variability. For the positive-CIE interval, these values average was fond to be 629 in BH-7, and 624 in BH-13. On the other hand, and again, a much lower values were observed for the pre-excursion and post-excursion intervals. These values were found to be 265 and 541 in BH-7, and 485 and 502 in BH-13 respectively.

**Discussion**

In this section, $\partial^{13}C_{org}$ stratigraphic profile generated here is to be correlated to their well documented counterparts from other parts of the world. Then, an expose is to be made about the lessons learned from this correlation, as they relate to the chronometric, biostratigraphic, and depositional implications.

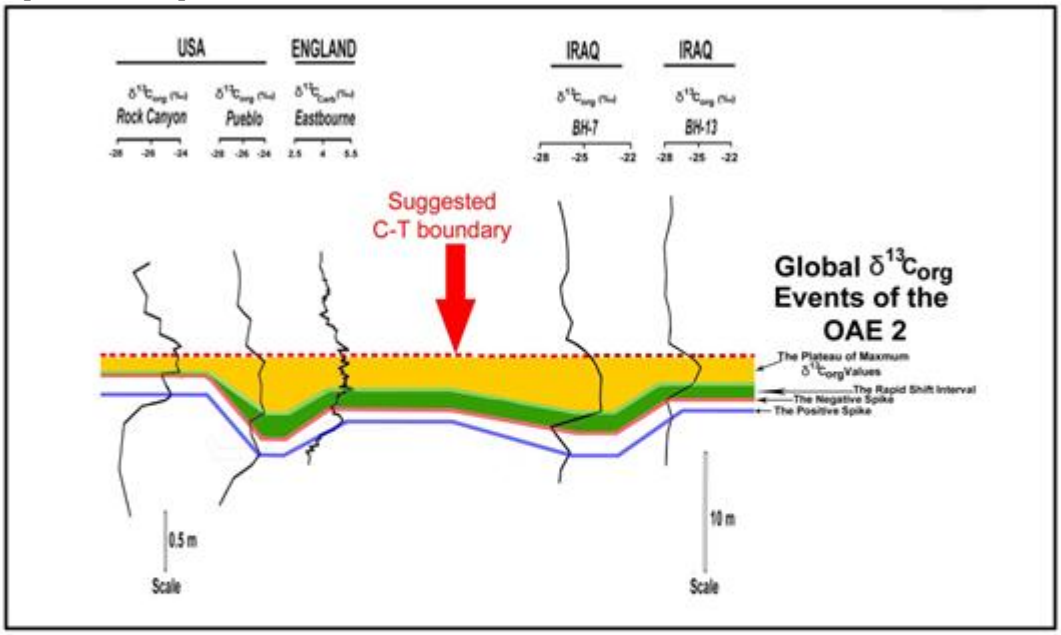


Figure 8. Correlation of ∂13Corg records from wells BH-7 and BH-13 with records from biostratigraphically well constrained OAE 2 profiles. ∂13Corg data for the Rock Canyon section are from [63] Pratt and Threlkeld, 1984; for the Pueblo section are from [22] Pratt,1985; for the Eastbourne section are from [64] Paul et al., 1999.

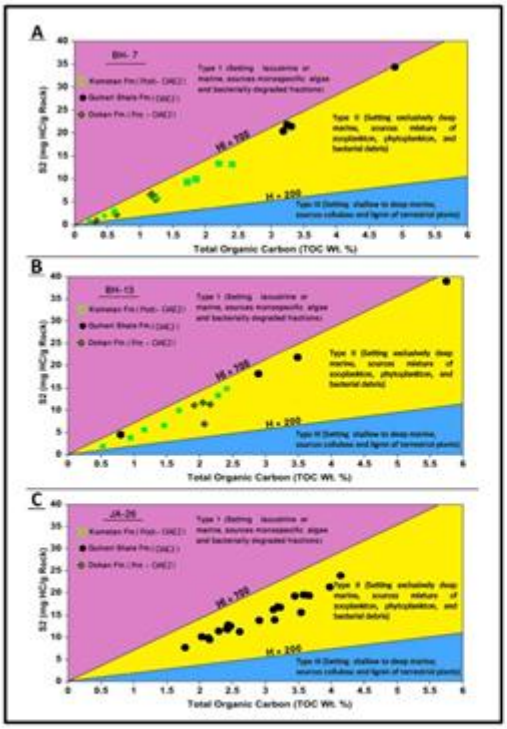


Figure 9. Plot of S2 verses TOC for samples from each well. A. for samples from BH-7; B. for samples from BH-13; C. for samples from JA-26.Adapted and modified after [65] Langford and Blanc-Valleron, 1990,

**Correlation**

Several authors e.g. [11-13] had put down an approximate age assignment for the Gulneri Shale Formation. Though these authors assignment were very close, a noticeable difference does still exist. These differences centers on the question of whether the deposition of the Gulneri shale had spanned the Cenomanian Turonian Boundary Interval (CTBI), or that this event had happened subsequently during the Early Turonian.

A globally well tested approach in resolving issues like the one at hand is to correlate the generated $\partial^{13}C_{org}$ curve with those already constructed from other parts of the world, wherein ultra high resolution biostratigraphic control had been established, which had been provided by diagnostic ammonites, bivalve, planktonic foraminifera, and calcareous nannofossils e.g. [21]. In this case, and in view of the available biostratigraphic data, the generated here in $\partial^{13}C_{org}$ curve was correlated with global reference curves already established for the Cenomanian Turonian Boundary Interval or the Global Oceanic Anoxic Event 2 (OAE 2). In so doing, $\partial^{13}C_{org}$ inflection points and gradient changes are used as a tie points for correlating all sections considered here.

The correlation framework is presented in Figures 8 and 10. In Figure 8, BH-7 and BH-13 $\partial^{13}C_{org}$ curves was correlated with other globally well established reference curves for the OAE 2 e.g. [22]. It can be seen that the correlation traverse line had started in the west from Pueblo in the US Midwest, which did happen to be the Global Boundary Stratotype Section and Point (GSSP) for the Cenomanian Turonian Boundary Interval CTBI), and to end up in the east in Iraq with wells BH-7 and BH-13. All the way through, the classical OAE 2 $\partial^{13}C_{org}$ excursion upward cycle of positive (the positive spike)-negative (the negative spike)-rapid shift (the negative spike to the base of the plateau)-positive (the plateau)-negative (return to pre-excursion values) had reproduced itself in all of the correlated profiles including those of BH-7 and BH-13.

Though that was the overall general picture, there still some slight differences as one move from one profile to another. The existence of such differences is not surprising in view of the fact that different parts of the world ocean had different sedimentation rates resulting in that some sections are thick while others are not. Another contributing factor is that different stratigraphic sections had different sampling densities. All of this had resulted in that some sections are having the pattern of saw tooth, while the other tends to be flat. Examples of the latter patterns are those of BH-7 and BH-13 wells, as well as that of Pueblo of the US Midwest. Nonetheless, this is not to undermine the statement

made above about the perfect match between BH-7 and BH-13 $\partial^{13}C_{org}$ systematics with those already well established for global OAE 2 reference curves.

The above statement is further corroborated by the containment of BH-7 and BH-13 OAE 2 dominated sections of significantly more of the organic matter expressed here as TOC percentage than the underlying and overlying sections Figures-4 and -5. In both wells, TOC percentage jumps from average background values of 0.43% in BH-7 and 1.53% in BH-13 to an average value of 2.73% in BH-7 and 3.14% in BH-13 throughout the OAE 2 dominated sections. This observation is consistent with trends reported for many of the OAE 2 global reference sections e.g. [23-25]. HI data which had been plotted in Figure-9, which add further support to this observation. From this figure, it can be seen that all the pertinent data had fallen in the field of type II, which indicate a marine origin of planktonic; zooplanktonic; and bacterial derivation for the studied samples organic matter e.g. [26]. As was the case before, this is another facet which is compatible with what is known from other OAE 2 sections e.g. [27-28].

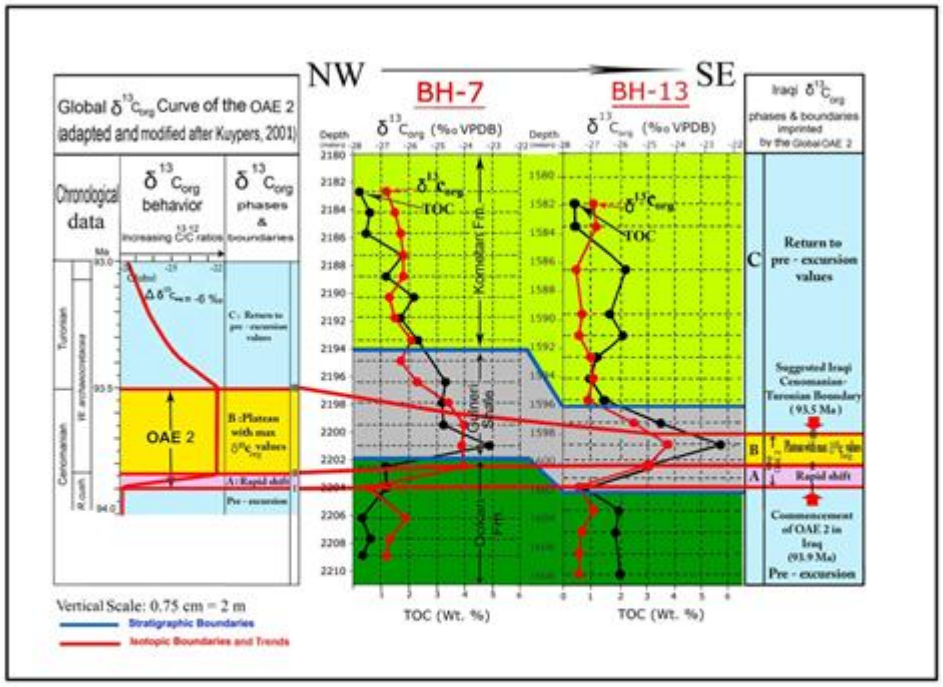


Figure 10. Correlation of ∂13Corg and TOC data of the studied samples from wells BH-7 and BH-13 with Kuypers's (2001) global ∂13Corg curve of the OAE 2. Adapted and modified after [29] Kuypers, 2001.

**Chronometric and biostratigraphic implications**

To further cement the case for the above statement, an alternative correlation scenario was presented in Figure 10, whereby BH-7 and BH-13 $\partial^{13}C_{org}$ curve is correlated to a smoothed OAE 2 global $\partial^{13}C_{org}$ curve, which a modified version for the one is presented by [29]. Again, the match between all the correlated profiles considered here is rather perfect. From this, it can be stated that the age of the studied samples including those of the Gulneri shale were indeed the Iraqi representatives of the Cenomanian Turonian Boundary Interval (CTBI), thereby supporting the point of view presented by [13].

Not only have that, but Figure 10 also helped in pinpointing the onset and termination of the OAE 2 in Iraq. The onset, and as was the case globally was placed at the level at which the negative spike was place e.g. [30-31]). This level did happen to be at depth of 2204.0 meter in BH-7, and at 1601.7 meter in BH-13. Because the consensus views that the OAE 2 onset was at 93.9 Ma [30-32], then these depths levels can be looked at it as the Iraqi 93.9 Ma timeline. On the other hand, OAE 2 termination was placed immediately above the end of the $\partial^{13}C_{org}$, signaling the start of what is called here as the post-excursion interval. In BH-7, this depth was at 2198.7 meter, while it was at 1598.0 meter in BH-13. Because OAE 2 termination was globally agreed on to be the Cenomanian Turonian Boundary (C\T Boundary) e.g. [33-37], then these depths levels can be considered as the Iraqi

Cenomanian Turonian Boundary, which happened at 93.5 Ma before the present e.g. [9], [38]. For many OAE 2 sections, high resolution faunal analysis was performed e.g. [39]. In general, it was fond that with the inception of the OAE 2 or with the impartation of the 93.5 Ma timeline all of the large keeled morphotypes of the planktonic foraminifera became extant. These to include clades like rotaliporids and dicarinellids. Upsection, the rest of the OAE 2 sections was fond to be dominated by dwarfed opportunistic fauna like heterohelicids, globogerinillids, and whitellineds. In addition, there should be a mention of what is called as the filament event. After OAE 2 termination at the Cenomanian-Turonian boundary or the 93.9 Ma timeline, large keeled planktonic foraminifera like dicarinillids and helvetoglobotruncanids reappear on the scene. The point to be made here is that the depth level counterparts of the 93.5 and 93.9 Ma timelines, and their interlude interval in BH-7 and BH-13 represents future targets of immense importance to be looked upon to see whether the global faunal variability was reflected in the local record as was already shown in $\partial^{13}C_{org}$ data, and to use the gained knowledge to further refine Iraq's chronostratigraphic framework.

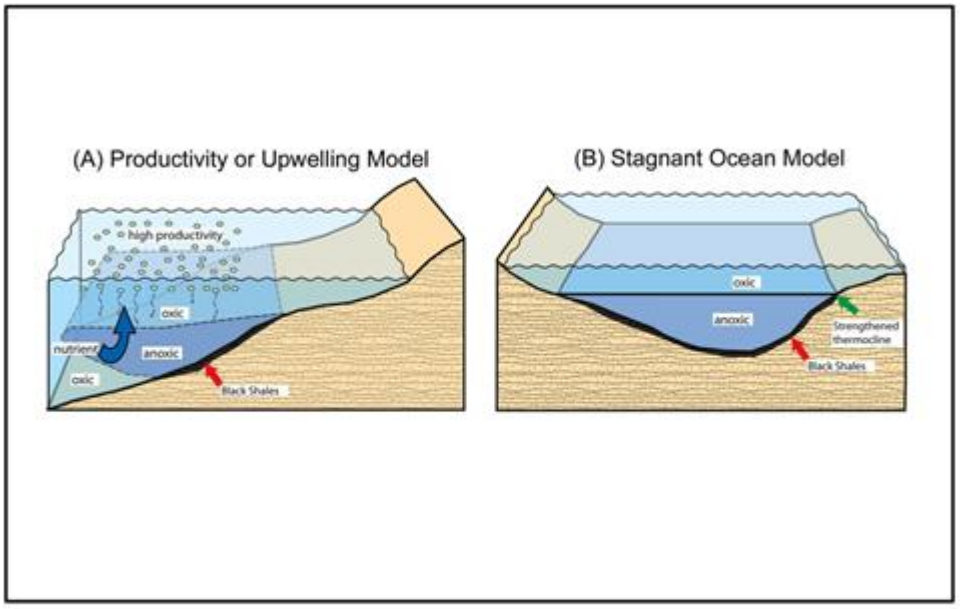


Figure 11. Conceptual models for the deposition of organic rich sediments like the Gulneri shale. Adapted and modified after [66] Takashimi et al., 2006.

**Depositional model**

In this section, a presentation to be made about where things standup on explaining how sediments like the Gulneri shale became so rich in organic matter. Afterwards an expose is to be made about how the Gulneri shale became so rich in organic matter within the context of the OAEs general model of formation.

**State of the art**

In view of the fact that in general $\partial^{13}C$ represent the isotopic ratio between $^{13}C$ and $^{12}C$, or in other word this ratio is between oxidized and reduced carbon, then $\partial^{13}C$ excursions and trends can be used as a proxy to infer the depositional condition under which the studied samples had been laid down e.g. [40], [41]. For instance, when $\partial^{13}C$ values skew positively, this was taken as evidence for enhanced burial of substantial amount of isotopically light $^{12}C$ enriched organic matter e.g. [7]. Because kinetic isotopic fractionation preferentially sequesters the light $^{12}C$ isotope into organic matter, the coeval seawater is lift to be enriched in the heavier $^{13}C$ isotope, which in turn is transpired to the concomitant depositing carbonate sediments and their contained organic matter by registering positive $\partial^{13}C$ excursion.

Having said so, the question which arises itself is what those conditions under which sediments become enriched are in organic matter like the Gulneri shale. Unfortunately, there is no simple answer to this corundum. However, there is in the literature a myriad of models each try to give an answer for the question at hand. In spite of this seemingly gray situation, two end members models had been oftenly invoked Figure-11. The first suggests increased marine biological productivity to be the

explanation e.g. [42], which is called the productivity model. The other model suggests increased anoxia associated with thermal or haline stratification as the reason for the organic matter enhanced preservation e.g. [43] which is called the preservation model.

To put things into a perspective, and according to [23] and [44], and references mentioned therein, ocean oxygen depletion or anoxia is the fundamental first step to inhibit decay of organic matter in both models, or in other word anoxia is the building stone for both models. In the context of the productivity model, increased primary production and the resultant excess $O_2$ consumption by the ever expanding biomass lead to anoxia [45]. In this model, and as in the words of [23], increased productivity was driven by increased continental nutrient runoff, which is brought about by elevated driven $CO_2$ temperatures, which in turn had increased evaporation, precipitation and weathering. While in the preservation model, anoxia is brought about by strong-water column stratification due to sluggish ocean circulation e.g. [45-46], thus preventing the down dwelling of oxygen enriched surface water. While the productivity model suggests that increased primary production, and the resultant excess $O_2$ consumption by the ever expanding biomass lead to anoxia [45].

However, and as it turns out, there is now widespread consensus that both of these models are in fact representing an intimately intertwined developmental phases within the OAEs course of evolution e.g. [7], [47].

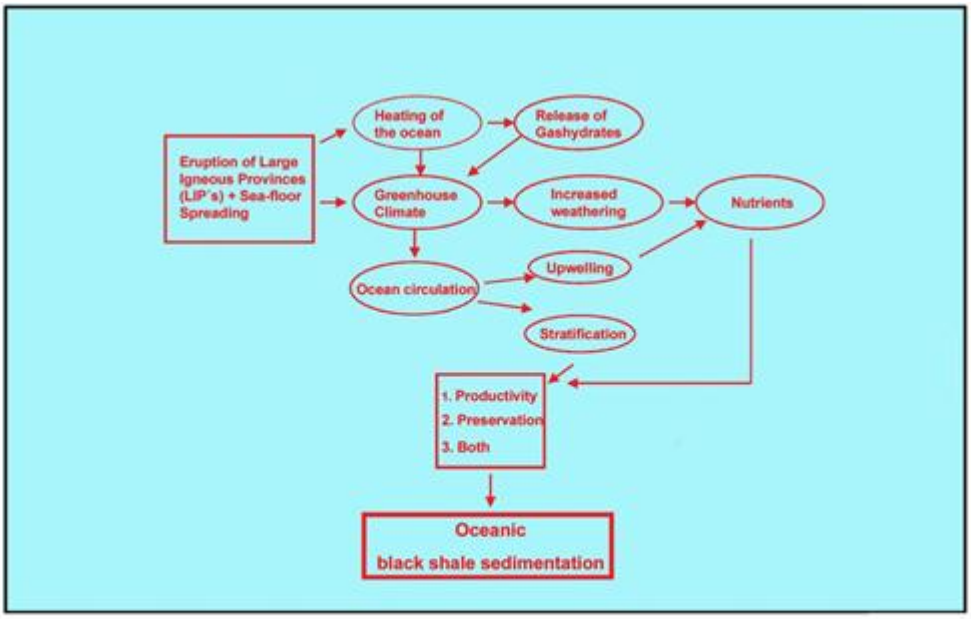


Figure 12. The generalized model for the inception; maintenance; and final termination of the OAEs. Adapted and modified after [67] Urbat, 2009.

**A close-up look at the Gulneri shale**

The forgoing discussion had made an excellent case for a cause and effect relationship between the global OAE 2 and the Gulneri shale characters, in particular the studied samples possession of Positive $\partial^{13}C_{org}$ and high TOC and HI values. In what will be becoming hereafter, an attempt is be made about how these samples came to acquire such characters. The discussion is be persuaded within the context of the OAEs general model, and whenever it is necessary, an elution to the OAE 2 relevancy is to be made. Figure-12 is an attempt for a graphical display of these words.

The consensus is that all OAEs inclusive of the OAE 2 are direct consequence of greenhouse or warm climate e.g. [48]. Because our planet is now in a glaciated status e.g. [49], one might wonder whether icehouse\greenhouse swings were common in deep times. Paleoclimatic proxies had testified repeatedly to this notion (e.g. [50], and many others).

These swings were interpreted to be in response to increasing\decreasing atmospheric concentration of a group of heat trapping gases Known as greenhouse gases (GHG) including water vapor, $CH_4$, $CO_2$ e.g. [51-52]. Because of its long residence time, the most potent of the GHG is $CO_2$ [53].The consensus is that atmospheric $CO_2$ concentration behavior was in response to variability in

global igneous activities, especially those associated with the emplacement of large Igneous Provinces (LIPs) e.g. [54]. In this context, it should be mentioned that OAE 2 triggering event was the emplacement of the Caribbean, Madagascar, and\or parts of the Ontong-Java Plateaux e.g. [55]. According to the latest estimates [56], these events increased paleo-$CO_2$ level by about 20% immediately before OAE 2 onset. Because magmatic $CO_2$ is known to be isotopically light, then the Guneri shale negative $\partial^{13}C_{org}$ spike is due to the injection of $^{13}C$ depleted by the OAE 2 magmatic driver e.g. [57-58].

Consequently, this pulse of global warming raises the temperature of already warm ocean [59]. As a result, the ocean revert to a status known as deoxygenating or anoxia, thereby the ocean is predisposed to have one of the OAEs [60]. According to [3], the causal link between oceanic warming and OAEs development include the following feedbacks: (1) reduced ventilation due to enhanced stratification and weakened circulation; (2) reduction of $O_2$ solubility; increased oceanic fertilization.

Due to the absence of life giving $O_2$, all $O_2$ breathing biomass become extant through a process known as mass extinction of existing biomass e.g. [4-6]. Because these biomass are the main grazer present in the water column, their absence enhances organic matter preservation. A corollary of this is the coeval sediments enrichment in organic matter, and their possession of positive isotope carbon $\partial^{13}C_{org}$ excursion as was manifested by the Gulneri shale rapid shift interval and plateau of maximum $\partial^{13}C_{org}$ values similar to what was well documented for other OAE 2 reference curves. As was mentioned earlier, this excursion is due to enhanced burial of $^{13}C$ depleted organic matter. Finally, as $CO_2$ atmospheric concentration dwindles via silicate weathering, and photosynthetic fixation, global temperature began to decrease [61]. When this trend is well established, oceans began to cool down. In response a cascade of biogeochemical feedbacks comes into play, through which the ocean once again regain its ability to absorb atmospheric $O_2$. And as time goes by, the oceans once again is to be bathed with well oxygenated water as was the case in pre-OAE 2 excursions. Consequently, oceanic water column is to be a habitable environment for $O_2$ breathing biomass. Therefore, this biomass is set on to graze and scavenges on much of the produced organic matter leading to the deposition of sediments with little or no organic matter, as was observed here in the post-excursion samples.

## Conclusions

Here below are the main conclusions arrived to, as well the recommendations for future work:-

1. The Gulneri shale is the Iraqi counterpart for the global OAE 2.
2. The age of the Gulneri shale ought to be bracketed as latest Cenomanian to earliest Turonian, or between 93.9 to 93.4 Ma before the present.
3. OAEs general model seems to account very well for the observed Gulneri shale $\partial^{13}C_{org}$ positive excursion, and its high TOC and HI values.

## Recommendations for future work

There is a need for future work to document the concentration and types of both anoxic and euxinic biomarkers, and redox sensitive elements. When these data become available at hand, then there will be at hand a better opportunity to establish a clearer picture about the oxygenation history of the Tethys Seaway in northern Iraq during the global OAE 2.

## Acknowledgement

The author would like to express his deepest gratitude to Professor Gerta Keller of Princeton University and Professor Thierry Adatte of the University of Lausanne for their indispensable help for this paper data acquisition schemes. The same goes to the Iraqi Ministry of Oil, and it is subsidiary North Oil Company. I also would like to thank the editorial board of the Iraqi Journal of Science, and their anonymous reviewers for their comments which greatly helped in improving this paper publishing quality.

## References

1. Schlanger, S.O., and Jenkyns, H.C., **1976**, Cretaceous oceanic anoxic events: Causes and consequences, *Geologie en Mijnbouw*, Vol. 55, PP. 179-184.
2. Owens, J.D., Jenkyns, H.C., Bates, S.M., Severnmann, S., Kuypers, M.M., Woodfine, R.G., and Lyons, T.W. **2013**, Sulfur isotopes track the global dynamics of euxinia during Cretaceous Oceanic Anoxic Event 2, Proceeding of the National Academy of Sciences, Vol. 110, PP. 18407-18412.

**3.** Paulmier, A., Ruiz-Pino, D., and Garcon, V. **2011**, $CO_2$ maximum in the oxygen minimum zone (OMZ), *Biogeosciences*, Vol. 8, PP. 239- 252.

**4.** Leckie, R.M., Bralower, T.J., and Cashman, R. **2002**, Oceanic anoxic events and plankton evolution: Biotic response to tectonic forcing during the mid-Cretaceous, *Paleoceanography*, Vol. 17, dol: 10. 1029, 2001 PAOOO623.

**5.** Erba, E., **2004**, Calcarous nannofossils and Mesozoic oceanic anoxic events, *Marine Micropaleontology*, Vol. 52, PP. 85-106.

**6.** Browing, E.L., and Watkins, D.K. **2008**, Elevated primary productivity of calcareous nannoplankton associated with ocean anoxic event I b during the Aptian Albian transition (Early Cretaceous), *Paleoceanography*, Vol. 23, PA2213, dol: 1029/2007 PA1413.

**7.** Jenkyns, H.C., **2010**, Geochemistry of oceanic anoxic events, *Geochemistry, Geophysics, Geosystems*, Vol. 11., PP. 1- 30, OO 3004, doi: 10. 1029/2009GCOO2788.

**8.** Jarvis, I., Lignum, J.S., Groecke, D.R., Jenkyns, H.C., and Pearce, M.A. **2011**, Black shale deposition, atmospheric CO drawdown, and cooling during the Cenomanian-Turonian Oceanic Anoxic Event, *Paleoceangraphy*, Vol. 26, PA32001.

**9.** Scott, R. W. A. **2014**, Cretaceous chronostratigraphic database: construction and applications, *Carntes de Geologie* [*Notebooks on Geology*], vol. 14, PP. 15-37.

**10.** Sinninigha Damste, J.S., Bentum, E.C., Reichart, G.J., Pross, J., and Schouten, S. **2010**, A $CO_2$ decrease- driven cooling and increased latitudinal temperature gradient during the mid-Cretaceous Oceanic anoxic Event 2, *Earth and Planetary Science letters*, Vol. 293, PP. 97-103, doi:10.1016/ j.epsl. 2010. 02.027, 2010.

**11.** Bellen, R. C. Van, Dunnington, H.V., Wetzel, R., and Morton, D.M. **1959**, Lexique Stratigraphique International, Centre National, de la Recherche Scientifique Asia, Fascicule, 10a- Iraq, Paris, Asia.

**12.** Abawi, T. S., Hammoudi, R.A., and Al- Khafaf, A.O. **2006**, Stratigraphy of the Gulneti Formation (Upper Cretaceous) in the Type section, Dokan Area, northeastern Iraq, *Iraqi Journal of Earth Scinences*, Vol. 6, PP. 33- 42.

**13.** Ameen, F. A., and Gharib, H. **2013**, Biostratigraphy of the Tethyan Cretaceous successions form northwestern Zagros fold-thrust belt, Kurdistan region, NE Iraq, *Arabian Journal of Geosciences*, Vol. 7, PP. 2689- 2710.

**14.** Dunnington, H. V. **1958**, Generation, migration, accumulation, and dissipation of oil in Northern Iraq in Habitat of Oil a Symposium edited by L. G. Weeks, American Association of Petroleum Geologists Special publication, PP. 1194-1251.

**15.** Henson, F. R. S. **1951**, Observations on the geology and petroleum occurrence of the Middle East, Third World petroleum Congress, The Hague, Proceedings Section 1, PP. 118-140.

**16.** Jassim, S. Z., and Goff, J.C. **2006**, *Geology of Iraq*, Dolin Publishers, the Czech Republic.

**17.** Ziegler, M. A. **2001**, late Permian to Holocene paleofacies evolution of the Arabian plate and its hydrocarbon occurrences, *Geo Arabia*, Vol. 6, PP. 445- 504.

**18.** Aqrawi, A. A. M., Goff, J.D., Horbury, A.D., and Sadooni, F.N. **2010**, *Petroleum Geology of Iraq*, Scientific Press ltd., the UK.

**19.** Keller, G., and Pardo, A. **2004**, Age and paleoenvironment of the Cenomanian-Turonian global stratotype section and point at Pueblo, Colorado, *Marine Micropaleontology*, Vol. 51, PP. 95-128.

**20.** Keller, G., Berner, Z., and Stueben, D. **2004**, Cenomanian-Turonian and $\partial^{13}C$ and $\partial^{18}O$, sea level and salinity variations at Pueblo, Colorado, *Marine Micropaleontology*, Vol. 211, PP. 19- 43.

**21.** Kennedy, W. J., Walasaczy, I., and Cobban, W.A. **2005**, The global boundary, stratotype section and point for the base of the Turonian stage of the Cretaceous, Pueblo, Colorado, USA, *Episodes*, Vol. 28, PP. 93- 104.

**22.** Pratt, L. M. **1985**, Isotopic studies of organic matter and carbonate in tocks of the Greenhorn marine cycle, In Fine- grained Deposits and Biofacies of the Cretaceous Western Interior Seaway: Evidence of cyclic sedimentary processes edited by L.M. Pratt, E. G. Kauffman, and F. B. Zelt, Society for Sedimentary Geology (SEPM), Field Trip Guidebook 4, PP. 38-48.

**23.** Mort et al. **2007**, Phosphorous and the roles of productivity and nutrient recycling during Oceanic Anoxic Event 2, *Geology*, Vol. 35, PP. 483-486.

**24.** Fernando et al. **2010**, Calcareous nannofossil biostratigraphy of the Thomel Level (OAE2) in the Lambruisse Vocontian, Southeast France, *Geobios*, Vol. 43, PP.45-57.
**25.** Reolid, M., Sanchez-Quinonez, C.A., Alegret, L., and Molina, E. **2015**, Paleoenvironmental turnover across the Cenomanian-Turonian transition in Oued Bahloul, Tunisia: Foraminifera and geochemical proxies, *Palaeogeography, Palaeoclimatology, Palaeoecology*, Vol. 417, PP. 491-510.
**26.** Tissot R.P. and Welte, D.H. **1984**, *Petroleum Formation and Occurrence*, Springer-Verlag, New York, 699 PP.
**27.** Scopelliti, G., Bellanca, A., Neri, R., Baudin, F., and R. Coccioni, R. **2006**, Comparative high-resolution chemostratigraphy of the Bonarelli level from the reference Bottanccione section (Umbria-Marche Apennines) and from an equivalents section in NW Sicily: Consistent and contrasting responses to the OAE2, *Chemical Geology*, Vol. 228, PP. 266-285.
**28.** Mort et al. *2008*, Organic carbon deposition and phosphorous accumulation during Oceanic Anoxic Event 2 in Tarfaye, Morocco, *Cretaceous Research*, Vol. 29, PP. 1008-1023.
**29.** Kuypers, M.M.M. **2001**, Mechanisms and biogeochemical implications of the Mid-Cretaceous global organic burial events, PhD thesis, Utrecht University, 135 PP.
**30.** Sageman, B.B., Meyers, S.R., and Arthur, M.A. **2006**, Orbital time scale and new C-isotope record for Cenomanian-Turoanian boundary stratotype, *Geology*, Vol. 34, PP. 125-128.
**31.** Meyers et al. **2012**a, Intercalibration of radioisotopes and astrochronologic time scales for the Cenomanian-Turonian boundary interval, Western Interior Basin, USA, *Geology*, Vol. 40, PP. 7-10.
**32.** Kuroda et al. *2007*, Contemporaneous massive subaerial volcanism and Late Cretaceous oceanic anoxic event 2, *Earth and Planetary Science Letters*, Vol. 256, PP. 211-223, doi: 10.1016j:epsl.2007.01.027.
**33.** Nederbragt, A., and Eiorentino, A. **1999**, Stratigraphy and Paleoceanography of the Cenomanian-Turonian boundary event in Qued Mellegue, northwestern Tunisia, *Cretaceous Research*, Vol. 20, PP. 47-62.
**34.** Gale et al. **2000**, Marine biodiversity through Late Cenomanian-Early Turonian: Paleoceanographic controls and sequence stratigraphic biases, *Journal of the Geological Society of London*, Vol. 157, PP. 745-757.
**35.** Tsikos et al. **2004**, Carbon isotope stratigraphy recorded by the Cenomanian-Turonian Oceanic Anoxic: correlation and implications based on three key localities, *Journal of the Geological Society of London*, Vol. 161, PP. 711- 719.
**36.** Fernando, A.G.S., Takashima, R., Nishi, H., Giraud, F., and Okada, H. **2010**, Calcareous nannofossils biostratigraphy of the Thomel level (OAE2) in the Lambruisse Section, Vocontian Basin, *Geobios*, Vol.43, PP.45-57.
**37.** Melinto- Dobrinescu, M.C., Bernardes, M.E., Kaiho, K., and Lamolda, M.A. **2013**, Cretaceous oceanic anoxic event 2 in the Arobes Section, northern Spain: nannofossil fluctuations and isotope events: In Isotopic Studies in Cretaceous Research, edited by A.V. Bojar, M.C. Melinte-Dobrinescu, and J. Smit, *Geological Society of London Special Publication*, Vol.382, PP.63-84.
**38.** Oggs, J.G., and Hinnov, L.A. **2012**, Cretaceous: In the *Geologic Time Scale* 2012, edited by F.M. Ogg, M.D. Schmitz, and G.M. Ogg, Elsevier Publication, PP. 793-854.
**39.** Takashima, R., Nishi, H., Hayasgi, K., Okasa, H., Kawashata, H., Yamanaska, T., Fernando, A., and Mampuku, M. **2004**, Litho-, bio-, and chemostratigraphy across the Cenomanian Turonian boundary (OAE2) in the Vocontian Basin of southeastern France, *Palaeogeography, Palaeoclimatology, Palaeoecology*, Vol. 273, PP. 61- 74.
**40.** Scholle, P.A., and Arthur, M.A., 1980, Carbon isotope fluctuations in Cretaceous pelagic Limestones: stratigraphic and Potroleum exploration tool, *American Association of Petroleum Geologists Bulletin*, Vol. 64, PP. 67-87.
**41.** Arthur, M.A., Pratt, W.E., and Pratt, L.M. **1988**, Geochemical and climatic effects of increased marine organic carbon burial at the Cenomanian/ Turonian boundary, *Nature*, Vol. 335, PP. 714-717.
**42.** Pedersen, T.F., and Calvert, S.E. **1990**, Anoxia and productivity what controls the formation of organic-carbon-rich sediments and sedimentary rocks? *American Association of Petroleum Geologists Bulletin*, Vol. 74, PP. 454-466.

**43.** Demaison, G.J., and Moore, C.T. **1980**, Anoxic environments and oil source beds genesis, *Organic Geochemistry*, Vol. 2, PP. 9-31.

**44.** Huck, S., Heimhofer, U., Rameil, N., Bodin, S., Immenhauser, A. **2011**, Strontium and carbon-isotope chronostratigraphy of Barremian-Aptian shoal-water carbonates: Northern Tethyan Platform drawing predates OAE1a, *Earth and Planetary Science Letters*, Vol. 304, PP. 547-558.

**45.** Erbacher, J.O., Huber, B.T., Norris, R.D., and Markey, M. **2001**, Increased thermohaline circulation as a possible cause for an Oceanic Anoxic Event in the Cretaceous Period, *Nature*, Vol. 409, PP. 325-327.

**46.** Schlanger, S.O.,and Jenkyns, H.C. 1976, Cretaceous oceanic anoxic events, Causes and consequences, *Geologie en Mijnbour*, Vol. 55, PP. 179-184.

**47.** Blumenberg, M., and Wiese, F. **2012**, Imbalanced nutrients as triggers for black shale formation in a shallow shelf setting during the OAE 2, (Wunstorf, Germany), *Biogeosciences*, Vol. 9, PP. 4139-4153.

**48.** Ozaki, K., and Tajika, E. **2013**, Biogeochemical effects of atmospheric oxygen concentration, phosphorous weathering, and sea level stand on oceanic redox chemistry: Implications for greenhouse climates, *Earth and Planetary Science Letters*, Vol. 373, PP. 129-139.

**49.** Montanez, I.P., and Poulsen, C.J. **2013**, The Late Paleozoic ice ages: an evolving paradigm, *Annual Review of Earth and Planetary Sciences*, Vol. 41, PP. 629-656, doi: 10.1146/annurev.earth. 031208.100118.

**50.** Bender, M.L. **2013**, *Paleoclimate* (Princeton Primers in Climate), Princeton University Press, 320 PP.

**51.** Vaughan, A.P.M. **2007**, *Climate and geology-a Phanerozioc perspective, In Deep-Time Perspectives on climate change: Marrying the signal from computer models and biological proxies*, edited by M. Williams, F.J. Gregory, and D.N. Schmidt, the Geological Society and the Micropaleontological Society, Special Publication, London, PP. 5-59.

**52.** Park, J., and Royer, D.L. **2011**, Geologic constraints on the glacial amplification of Phanerozoic climate sensitivity, *American Journal of Science*, Vol. 311, PP. 1-26.

**53.** Huang, T.H., Fu, Y.H., Pan, P.Y., and Chen, C.T.A. **2012**, Fluvial carbon fluxes in tropical rivers, *Current Opinion in Environmental Sustainability*, Vol. 4, PP. 179-185, doi: 10.1016/j.cosust 2012.02.003.2012.

**54.** Bond, D.P.G., and Wignall,P.B. **2014**, Large igneous provinces and mass extinctions: an update, 505, Geological Society of America, PP. 29-55, doi: 10.1130/2014, 2505.(02).

**55.** Erba, E., Duncan, R.A., Tiraboschi, C., Weissert, D., Jenkyns, H., and Malinerno, A. **2015**, A Environmental Consequences of Ontong Jaqa Plateau and Kerguelen Plateau Volcanism, *American Geological Society Paper*, Vol. 511, doi: 10.1130/20152511(15).

**56.** Wang, Y., Huang, C., Sun, B., Quan, C., Wu, J., and Lin, Z. **2014**, Paleo-$CO_2$ variation trends and the Cretaceous greenhouse climate, *Earth-Science Reviews*, Vol. 129, PP. 136-147.

**57.** Keller, G., Adatte, T., and Burns, S.J. **2001**, Paleoenvironment of the Cenomanian-Turonian transition at Eastborne, England, *Cretaceous Research*, Vol. 22, PP. 391-422, doi: 10. 1006/cres.2001.0264.

**58.** Hansen, H.J. **2006**, Stable isotopes of carbon from basaltic rocks and their possible relation to atmospheric isotope excursion, *Lithos*, Vol. 92, PP. 106-116.

**59.** Stanley, S.M. **2010**, Relation of Phanerozoic stable isotope excursion to climate, bacterial metabolism, and major extinctions, PNAS, Vol. 107, PP. 19185-19189.

**60.** Wignall, P.B., **2001**, Large igneous provinces and mass extinctions, *Earth Science Review*, Vol. 53, PP. 1-33.

**61.** Pogge von Strandmann, P.A.E., Jenkyns, H.C., and Woodfine, R.G. **2013**, Lithium isotope evidence for enhanced weathering during Oceanic Anoxic Event 2, *Nature Geoscience*, Vol. 6, PP. 668-672, doi: 1038/ngeo1875.

**62.** Fox, J.E. and Albrandt, T.S. **2002**, Petroleum Geology and Total Petroleum Systems of the Widyan Basin and Interior Platform of Saudia Arabia and Iraq, United States Geological Survey Bulletin, Report Number B, 2202.

**63.** Pratt, L.M., and Threlkeld, C.N. **1984**, Stratigraphic significance of $^{13}C\backslash^{12}C$ ratios in Mid-Cretaceous rocks of the Western Interior, U.S.A., In the Mesozoic of Middle North America edited by D.F. Stott, and D.J. Glass, PP. 305-312, Canadian Society of Petroleum Geologists.

**64.** Paul et al. **1999**, The Cenomanian-Turonian boundary at Eastbourne (Sussex, UK): a proposed European references section, *Palaeogeography, Palaeoclimatology, Palaeoecology*, Vol. 150, PP. 83-121.

**65.** Langford, F.F., and Blanc-Valleron, M.-M. **1990**, Interpreting Rock-Eval pyrolysis data using graphs of pyrolizable hydrocarbons vs. total organic carbon, *American Association of Petroleum Geologists Bulletin*, Vol. 74, PP. 799-804.

**66.** Takashima, R., Nishi, H., Huber, B.T., and Leckie, R.M. **2006**, Greenhouse world and the Mesozoic Ocean, *Oceanography*, Vol. 19, PP. 64-74.

**67.** Urbat, I., **2009**, Oceanic Anoxic Event (OAE) 1b: High resolution geochemical studies, Mazagan Plateau and Vocontian Basin, PhD Thesis, Universidad zur Koln.